Available online at www.sciencedirect.com
ScienceDirect
Trans. Nonferrous Met. Soc. China 31(2021) 2899−2908
Transactions of Nonferrous Metals Society of China
www.tnmsc.cn

Effect of non-isothermal aging on microstructure and properties of Al−5.87Zn−2.07Mg−2.42Cu alloys

Yao LI[1], Guo-fu XU[1,2], Xiao-yan PENG[1], Shi-chao LIU[1], Ying DENG[1], Xiao-peng LIANG[1]

1. School of Materials Science and Engineering, Central South University, Changsha 410083, China;
2. Key Laboratory of Nonferrous Metal Materials Science and Engineering of Ministry of Education, Central South University, Changsha 410083, China

Received 9 November 2020; accepted 10 August 2021

Abstract: The evolution of microstructure and properties of Al−5.87Zn−2.07Mg−2.42Cu alloys during non-isothermal aging was studied. The mechanical properties of the alloy were tested by stretching at room temperature. The results show that in the non-isothermal aging process, when the alloy is cooled to 140 °C, the ultimate tensile strength of the alloy reaches a maximum value of 582 MPa and the elongation is 11.9%. The microstructure was tested through a transmission electron microscope, and the experimental results show that the GP zones and η' phases are the main strengthening precipitates. At the cooling stage, when the temperature dropped to 180 °C, the GP zones were precipitated again. Besides, the experimental results show that the main strengthening phase during non-isothermal aging is η' phases.

Key words: Al−Zn−Mg−Cu aluminum alloy; non-isothermal aging; η' phases; mechanical properties

1 Introduction

Al−Zn−Mg−Cu alloy has been widely used in transportation and aerospace due to its low density, high specific strength and good plastic processing performance [1−4]. As one of the important applied materials in the aerospace industry, the comprehensive performance of Al−Zn−Mg−Cu alloy will face major challenges. In order to keep up with the development of aerospace, transportation and military technology, high strength, high toughness and good corrosion resistance are the development trends and important research directions of the Al−Zn−Mg−Cu alloy. These properties depend on the state of the structure, including not only the grain morphology, grain size and grain boundary configuration, but also the type, morphology, size, quantity and distribution of precipitates. As a heat-treatable and strengthened aluminum alloy, the heat treatment process system is directly related to the structure of the alloy, thereby affecting the comprehensive performance of the material. Therefore, it is of great significance to continuously study the heat treatment process of aluminum alloys and to control the microstructure by improving the heat treatment system.

The main strengthening mode of the Al−Zn−Mg−Cu alloy is precipitation strengthening, and the strengthening effect depends on the type, size, quantity and distribution of precipitates. For these heat-treated alloys, aging treatment plays an important role in improving the strength and corrosion properties. Therefore, many aging systems have been exploited to improve the comprehensive performance of the alloy [5,6]. At present, peak-aging (T6), over-aging (T7X) and regression−re-aging (RRA) have been widely used in 7xxx Al alloys [7]. Traditional T6 alloys have high strength but low corrosion resistance [8]. T7X

Corresponding author: Xiao-peng LIANG, Tel: +86-18684894344, E-mail: liangxp@csu.edu.cn
DOI: 10.1016/S1003-6326(21)65701-1

alloys sacrifice some of the strength while improving corrosion resistance [9]. RRA alloys have a high comprehensive performance, but short-term high temperature regression treatment limits their use on large components [10]. The non-isothermal aging (NIA) system is a new aging process that can effectively regulate the precipitation behavior of the second phase by adjusting parameters such as temperature and heating velocity during the non-isothermal heating process. Recent studies have shown that NIA treatment of large components can simultaneously achieve high mechanical properties and superior corrosion performance. JIANG et al [11] studied the effect of NIA on the properties and corrosion behavior of Al−Zn−Mg−Cu alloy. It was found that proper reduction of the cooling rate can effectively improve the corrosion resistance of alloy, but the alloy strength declines obviously. LIU et al [12] studied the effect of repeated NIA treatment on the microstructure and properties of Al−Zn−Mg−Cu alloy. It was found that after repeated NIA treatment, the corrosion resistance was improved and the strength did not decrease significantly. PENG et al [13] studied the precipitation behavior of Al−Zn−Mg−Cu alloy during NIA. It was found that the size and volume fraction of precipitates increased with the increase of aging temperature.

However, in different non-isothermal aging systems, the precipitation type, precipitation order and size of Al−Zn−Mg−Cu alloy strengthening phases may be different, and thus the strengthening effect of the alloy is also different. Therefore, in this work, the changes in structure and properties of Al−Zn−Mg−Cu alloy were mainly studied during NIA.

2 Experimental

The material used in this work was taken from the forging engine connecting rod on the aircraft, as shown in Figs. 1(a). The sampling position and sample size are shown in Figs. 1(b) and (c), respectively. The alloy composition is Al−5.87Zn−2.07Mg−2.42Cu−0.1Mn−0.10Zr−0.11Fe−0.16Si (wt.%). Schematic diagram of heat treatment of the experimental sample is shown in Fig. 2. The sample was first subjected to solution treatment at 475 °C, 1 h and directly subjected to water quenching. During the NIA, the sample was first heated from 100 to 190 °C at a heating rate of 20 °C/h, and then reduced to 100 °C at a rate of 40 °C/h. The heating and cooling rates are adjusted by the power knob on the aging resistance furnace. When a sample was taken out every 10 °C, water cooled quickly. When the sample was heated or cooled to the target temperature, the sample was named HX or CX (for example, when the sample is heated to 120 °C, it is named H120, as shown in Fig. 2). The room temperature tensile test was carried out on an MTS 810 test machine at a stretching rate of 2 mm/min, and the experimental results were the average of three parallel samples. G2F20 transmission electron microscope (TEM), operating at 200 kV, was used to observe the evolution of microstructure. The TEM sample was mechanically thinned to less than 80 μm and then electropolished in 75% methanol and 25% nitric acid solution at temperatures between −30 and −20 °C. In addition, the size of precipitates was acquired by the Image-pro Plus software and the average size was counted among 100 precipitates.

3 Results

3.1 Mechanical properties

Figure 3 shows the strength and elongation distribution of the Al−Zn−Mg−Cu alloy during the NIA. It can be clearly seen that at the heating stage, the yield strength (YS) and ultimate tensile strength (UTS) of the alloy gradually increase and the elongation rate drops from 19.3% to 15.5% as the

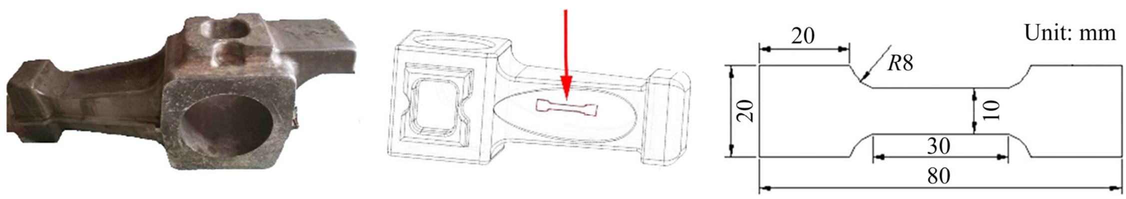

(a) (b) (c)

Fig. 1 Alloy sampling diagrams: (a) Original part drawing; (b) Sampling position diagram; (c) Tensile test diagram

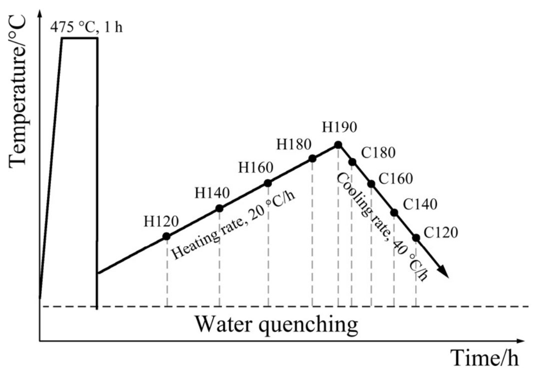

Fig. 2 Schematic diagram of heat treatment during non-isothermal aging

temperature increases. When the temperature rises to 190 °C, the UTS and YS of the alloy are enhanced to 570 and 501 MPa, respectively. During the cooling stage, the strength of the alloy shows a downward trend. When the temperature declines to 180 °C, the strength drops by 5 MPa. As the aging temperature continues to decrease, the strength begins to rise again. When the temperature drops to 140 °C, the alloy strength reaches the maximum, which is 582 MPa and the elongation reaches a minimum of 11.9%. As the temperature decreases further, the alloy strength shows a downward trend once again.

3.2 Microstructures

Figures 4 and 5 show the precipitate distribution and size of Al−Zn−Mg−Cu alloy after the NIA. It can be clearly seen that in the process of NIA, the precipitates are dispersed in the matrix. When the temperature rises to 140 °C, the size of precipitates, which is approximately 3.5 nm (Fig. 5), is significantly smaller than that of the precipitates in other conditions, and the density of the precipitates is also lower. When the temperature rises to 180 °C, precipitates of the alloy have grown apparently, reaching a maximum of 7.5 nm

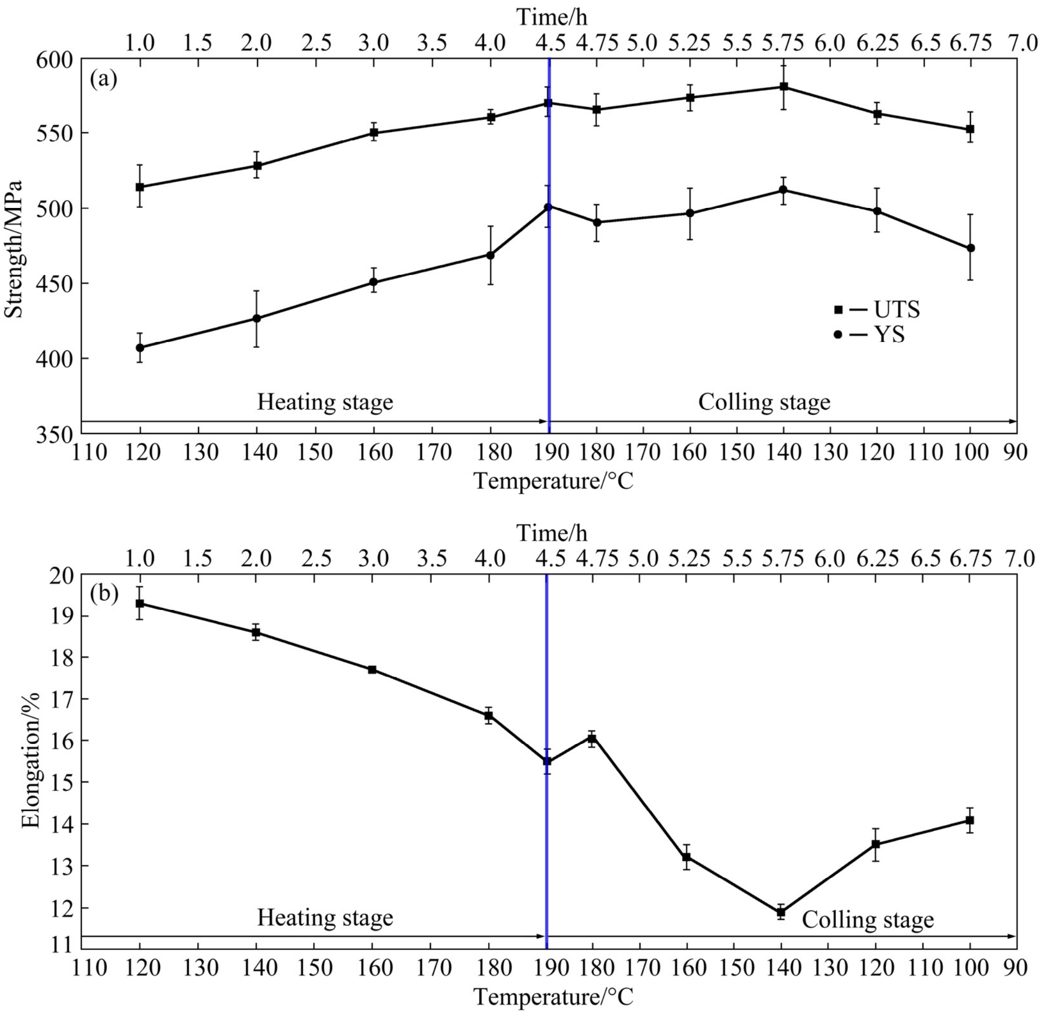

Fig. 3 Mechanical properties of strength (a) and elongation (b) of Al−Zn−Mg−Cu alloy after NIA treatment

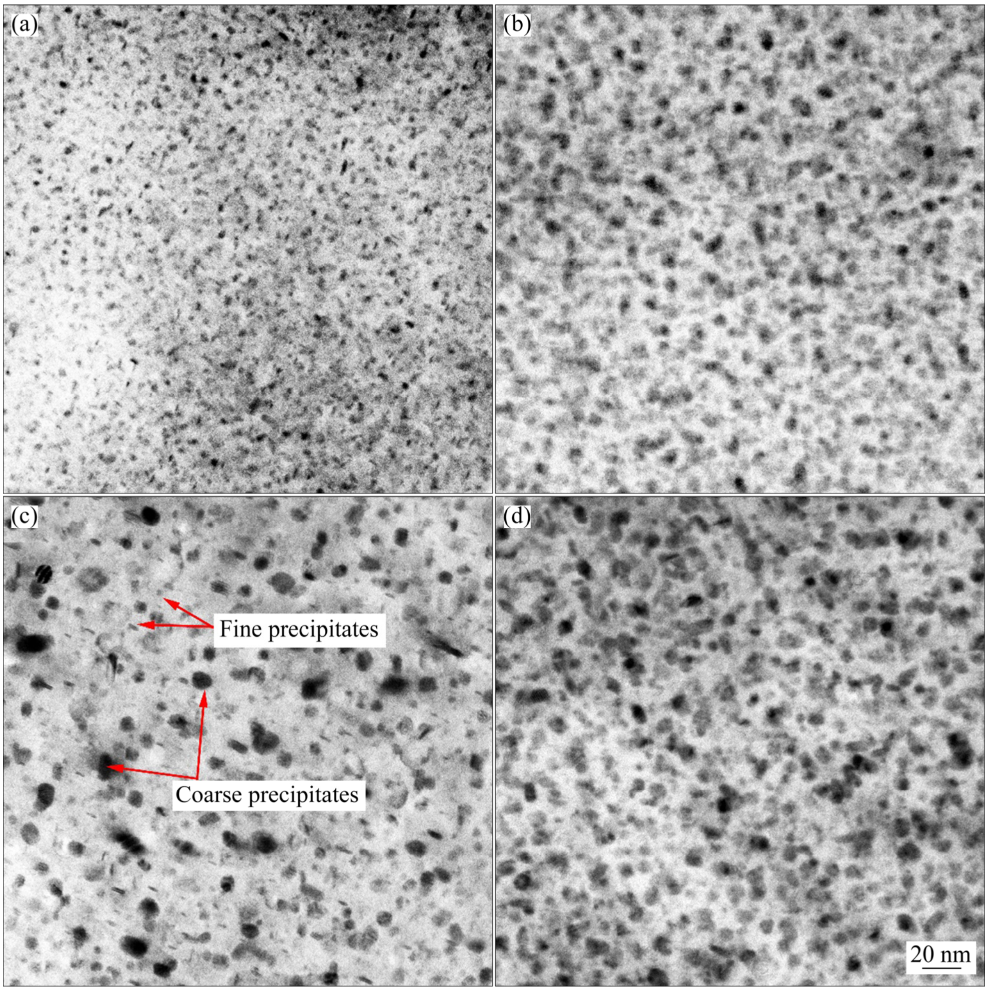

Fig. 4 Distribution of precipitates of Al−Zn−Mg−Cu alloy at different stages after NIA treatment: (a) H140; (b) H180; (c) C180; (d) C140

and the average size of precipitates is 5.6 nm (Fig. 5(b)). At the cooling stage, when the temperature drops to 180 °C, the density of the precipitates decreases significantly, and the large-scale precipitates and some fine precipitates can be clearly observed, as shown in Fig. 4(c). The maximum precipitates size can reach 13.5 nm, while the minimum precipitates size is only 1.9 nm, and the average size is 6.2 nm (Fig. 5(c)). When the aging temperature continues to drop to 140 °C, it can be clearly seen that the previous fine precipitates have grown up, the smallest size also reached 3.9 nm, and the average size reached 6.8 nm.

Figure 6 shows the selected-area diffraction patterns (SADPs) of Al−Zn−Mg−Cu alloy at different stages after NIA treatment. It can be seen from Fig. 6 that when the alloy is heated to 140 °C, the main precipitates are GP zones. When the temperature rises to 180 °C, precipitates grow obviously, as shown in Fig. 5(b), which are mainly η' phases (Fig. 6(b)). At the cooling stage, when the temperature decreases to 180 °C, two kinds of precipitates with completely different sizes are obviously precipitated in the alloy (Fig. 5(c)), which are mainly GP zones and η' phases, as shown in Fig. 6(c). When the alloy continues cooling down to the C140 state, fine precipitates in the C180 state grow up, and main precipitates in the alloy are η' phases (Fig. 6(d)).

Figure 7 shows the grain boundary precipitates distribution of Al−Zn−Mg−Cu alloy after the NIA treatment. It can be clearly seen that the grain boundary precipitates (GBPs) of the H140 alloy are fine and continuous. As the aging temperature continues rising to 180 °C, it can be seen from Fig. 7(b) that the grain boundary precipitates grow significantly, but they remain continuously

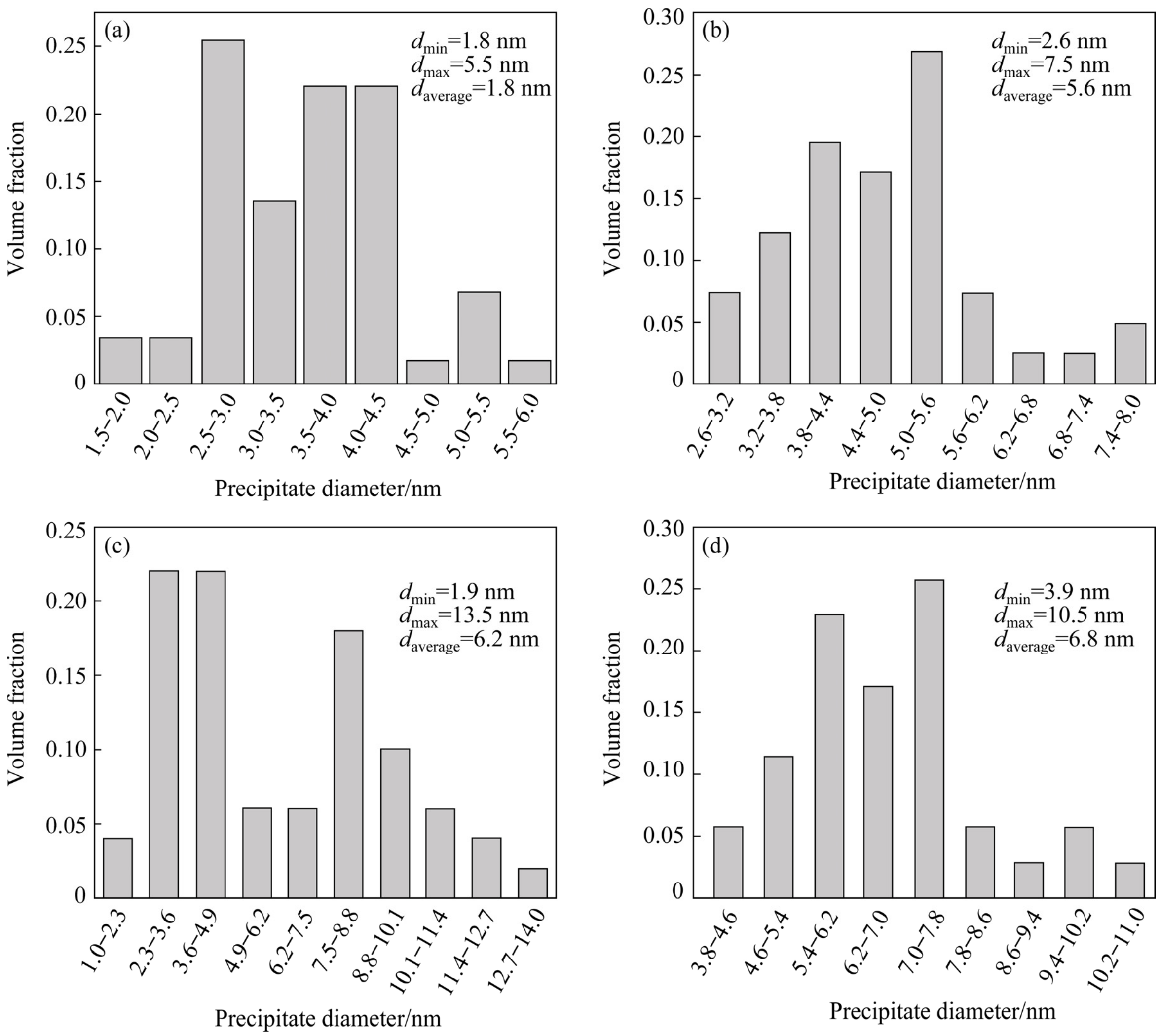

Fig. 5 Sizes of precipitates of Al−Zn−Mg−Cu alloy at different stages after NIA treatment: (a) H140; (b) H180; (c) C180; (d) C140

distributed. However, for the C180 alloy, a clear precipitate-free zone (PFZ) can be observed, the PFZ width reaches 21.9 nm, and the grain boundary precipitates spread discontinuously. When the temperature continues dropping to 140 °C, PFZ disappears while the grain boundary precipitates become continuous again and the precipitates are coarser.

4 Discussion

4.1 Effect of NIA treatment on precipitates

In general, the precipitation sequence of the precipitates of 7xxx aluminum alloy follows this order [13−15]: α-supersaturated solid solution → GP zones → η' → η ($MgZn_2$). Compared with the traditional aging heat treatment, the NIA treatment is significantly different. During the aging process, the influencing factors such as the nucleation driving force, the element's diffusion energy, and the nucleation critical condition will change significantly at different stages of aging [16]. Therefore, the precipitation process of multiple precipitates may be activated simultaneously during NIA [17]. Among them, the driving force (Δg) for precipitation of the alloy at a certain stage in the aging process can be described as [18]

$$\Delta g=-\frac{kT}{v_{at}}\ln\left(\frac{C}{C_{eq}}\right) \tag{1}$$

where v_{at} is the atomic volume of the precipitate (considered as constant for all samples), k is the Boltzmann's constant, T is the thermodynamic temperature, C_{eq} is the equilibrium solute concentration of the matrix, and C is the current solute concentration of the matrix.

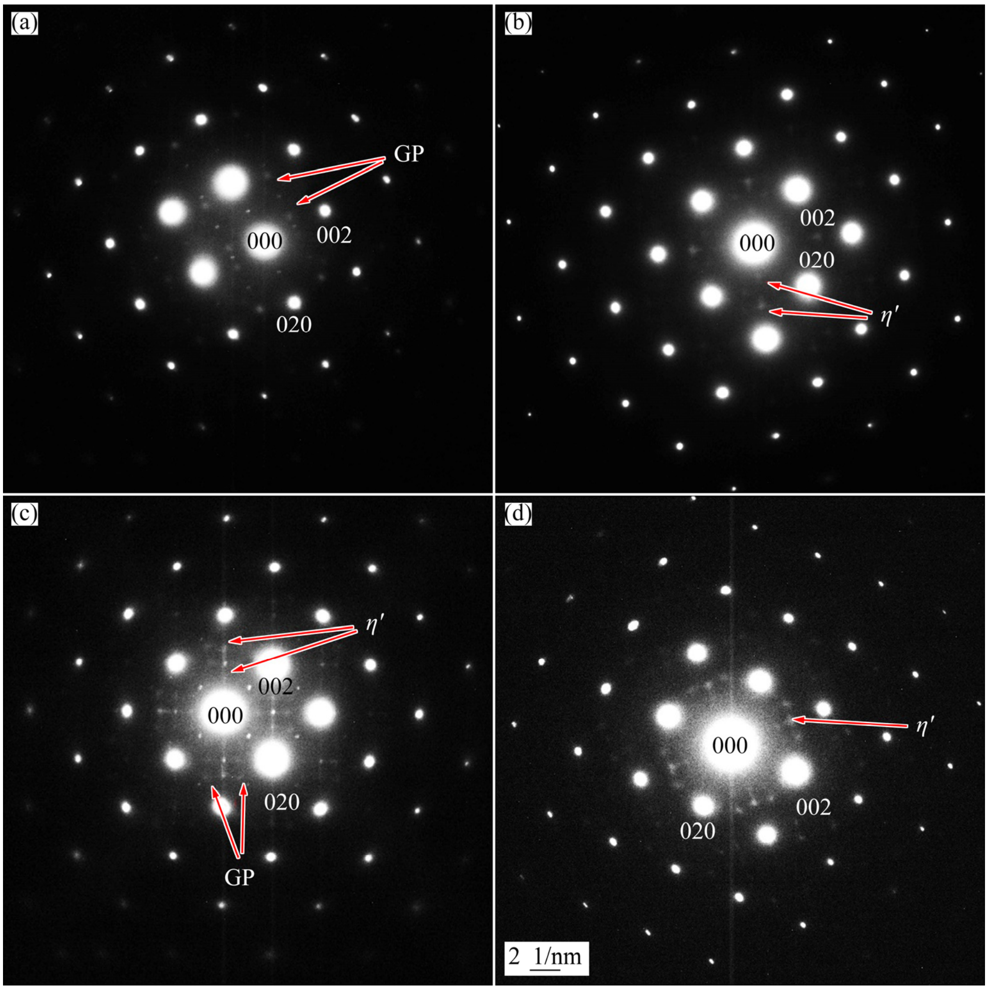

Fig. 6 SADPs of Al−Zn−Mg−Cu alloy at different stages after NIA treatment: (a) H140; (b) H180; (c) C180; (d) C140

Not only the nucleation and growth of precipitate relies on the Δg, but also the critical nucleation radius of the precipitate will determine whether the precipitate can grow up. The critical nucleation radius (R^*) can be described as [18]

$$R^*=\frac{2\gamma v_{\mathrm{at}}}{kT\ln(C/C_{\mathrm{eq}})} \tag{2}$$

where γ is the interfacial energy between precipitate and matrix.

According to the model proposed previously [18], the evolution of precipitates during the aging process depends on the size of precipitates relative to the R^*. The precipitates whose radius larger than the R^* will grow up, otherwise, they will dissolve. This theory is also suitable for the evolution of precipitates during NIA [19].

In this work, the temperature is constantly changing during the entire aging process, and this will directly affect the Δg of the alloy, and thus affect the nucleation process of precipitates. With the increase of the aging temperature, the Δg gradually increases, and the precipitates are more easily precipitated in the matrix. In addition, the growth of precipitates is also closely related to the R^*. As the aging temperature increases, the R^* gradually expands. In the non-isothermal aging process, when the temperature rises from 100 to 140 °C, the Zn and Mg atoms in the alloy segregate to form GP zones. Although the aging temperature is relatively low and the time is approximately short, due to the low nucleation barrier at the grain boundary, small continuous precipitates can be clearly observed at the grain boundary (Figs. 4(a) and 6(a)). With the increase of temperature, the Δg increases, the nucleation sites of the precipitates in the crystal increase, and the existing precipitates grow up at the same time, and the density and volume fraction of the precipitates are greatly

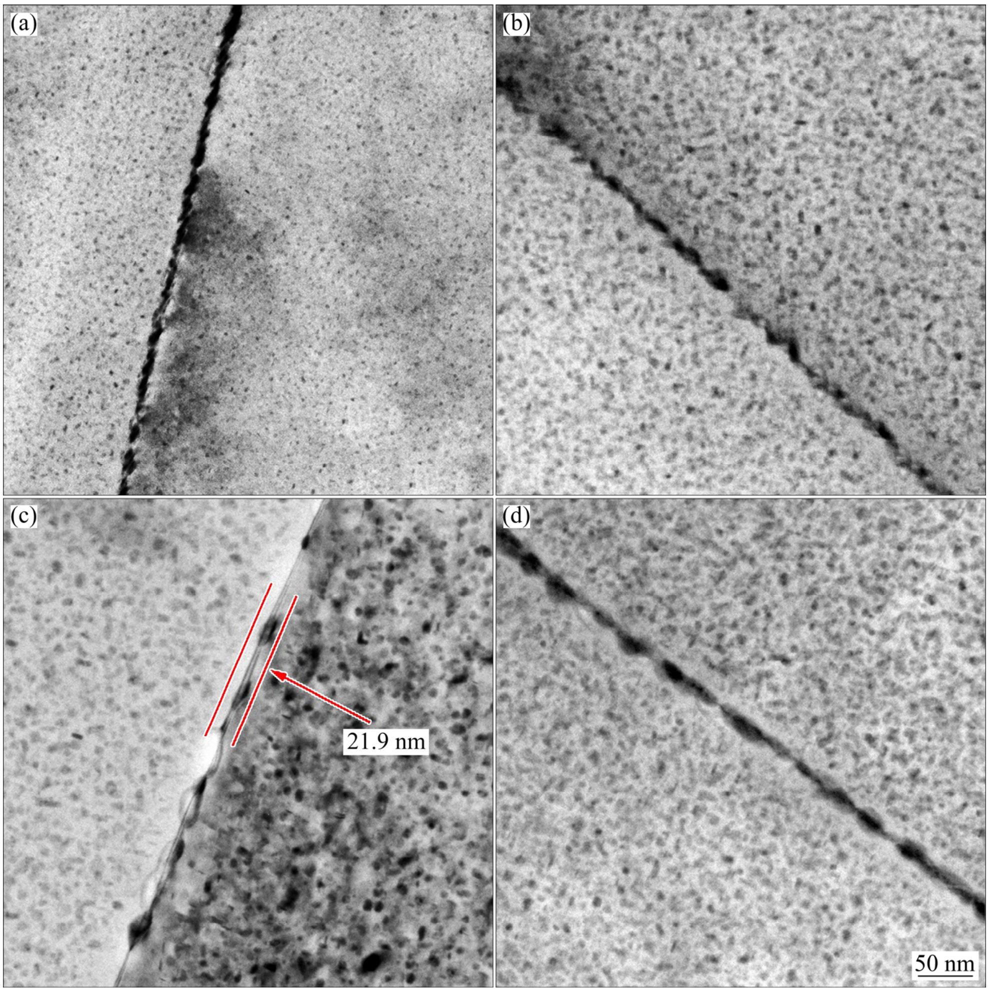

Fig. 7 TEM images of grain boundary precipitates of Al−Zn−Mg−Cu alloy at different stages after NIA treatment: (a) H140; (b) H180; (c) C180; (d) C140

increased. The precipitates in the matrix are mainly η' phase (Fig. 6(b)). The GBPs at the grain boundaries grow faster and are continuously distributed, but PFZ has not yet appeared near them. During the temperature rising period, the size of precipitates grew from an average of 3.5 nm (H140) to 5.6 nm (H180). The temperature continued increasing to 190 °C and then dropping to 180 °C. Since the alloy has experienced high temperature, the precipitates smaller than R^* in the alloy are dissolved and those larger than R^* grow and coarsen, and the density of the precipitates decreases. Due to the short aging time at the high temperature stage, the intracrystalline precipitates are dominated by the larger η' phases. The growth rate of GBPs accelerates, and the adjacent fine precipitates dissolve, forming a poor zone of solute atoms near the grain boundary, namely PFZ (Fig. 7(c)). At the cooling stage, due to the decrease in temperature, the Δg is relatively small, and R^* decreases. At this time, there are obviously fine precipitates in the alloy, and the minimum size reaches 1.9 nm. However, because the entire aging process is a continuous process, the size of precipitates that grow up during the heating phase is larger than R^*, and they will not dissolve back into the matrix as the aging temperature decreases, so the average size of overall precipitates still reaches 6.2 nm (C180). With the further decrease of the aging temperature to 140 °C, the growth rate of the large size η' phase slows down, so that the coarsening rate is controlled, driving new fine phases to nucleate and precipitate continuously, but the GBPs still coarsen and arrange intermittently. During the cooling process, the solubility of solute atoms in the PFZ region also decreases, and the secondary precipitates move from the boundary between the matrix and PFZ to the grain boundary, so PFZ becomes narrower or even disappears. Since the temperature is still higher than the peak aging temperature of the 7xxx aluminum alloy, fine precipitates of the secondary precipitation still grow up, as shown in Fig. 4(d), the average size of precipitate reaches 6.8 nm (C140).

4.2 Effect of precipitation on mechanical properties of alloys

The strengthening mechanism of Al−Zn−Mg−Cu alloy is mainly precipitation strengthening, which is mainly composed of the shearing mechanism and the Orowan strengthening mechanism. The shearing mechanism is a kind of mechanism that increases the strength of the alloy by dislocation shearing the second phase [20]. Orowan strengthening means that when the size of the precipitated phase reaches a certain level, dislocations can only bypass the second phase, thereby increasing the strength of the alloy to a certain extent [21]. In this study, the strengthening mechanism of the alloy is mainly based on the shearing mechanism due to the smaller size of precipitates. For those precipitates of smaller size, which will hinder the movement of dislocations, but dislocations can pass them by shearing, thus improving the alloy strength $\Delta\sigma_A$, which can be expressed as [22]

$$\Delta\sigma_A=c_1 f^{m} d^{n} \tag{3}$$

where f is the volume fraction of the precipitates, d is the diameter, and c_1, m, and n are regarded as constants.

As the aging temperature increases, precipitates become coarser gradually and dislocations can only bypass them. Then, the alloy strength $\Delta\sigma_B$ is given as [23]

$$\Delta\sigma_B=c_2 f^{1/2} d^{-1} \tag{4}$$

where c_2 is a constant. In this case, as the size of the precipitates increases, the strength decreases.

Therefore, the competition between the sizes of the precipitated phases determines the properties of the alloy. By rationally adjusting the aging temperature, the size of the precipitates can be effectively controlled, and finally the alloy properties are improved. As shown in Figs. 4 and 5, during the aging temperature increasing stage, when the aging temperature increases from 140 to 180 °C, the precipitates are significantly coarsened, and the average size increases from 3.5 to 5.6 nm. When the temperature further increases to 190 °C, in order not to further coarsen the precipitates, a reasonable choice of temperature reduction can effectively control the size of the precipitates, thereby maintaining the performance of alloy at a certain level. As shown in Fig. 5(a), when the alloy is aged at 140 °C, the maximum size of precipitates is 5.5 nm. At this time, precipitates can effectively hinder the movement of dislocations, cutting the dislocations through the precipitated phase, requiring a certain amount of stress, which improves the alloy properties. When the aging temperature further increases to 180 °C, the precipitates grow significantly, the maximum size reaches 7.5 nm, and the minimum size is 2.6 nm, but the average precipitates size is only 5.6 nm, indicating that the strengthening mechanism of the alloy at this time is mainly the shearing mechanism.

At the cooling stage, when the temperature decreases to 180 °C, it can be seen from Fig. 4 and Fig. 6(c) that there are small-sized GP zones inside the alloy. The minimum size of precipitates reaches 1.9 nm, and the average size is 6.2 nm. At this moment, dislocations are still dominated by cuts. However, when dislocations are cut through secondary precipitated GP zones, the required stress is small, so the alloy properties are reduced, as shown in Fig. 3. When the aging temperature further decreases to 140 °C, the original secondary precipitated GP zones grow into η' phases. At this time, the minimum precipitates size is 3.9 nm, and the average is 6.8 nm. In addition, it can be seen from Figs. 4(c) and (d) that when the temperature drops to 140 °C, the precipitated phase density increases significantly. Furthermore, it can be seen from Fig. 5(d) that the size distribution of the precipitated phases is mainly small-sized precipitated phases, so the strength of the alloy reaches the maximum at this time.

5 Conclusions

(1) During NIA treatment, the GP zones and η' phases are the main strengthening precipitates. At the cooling stage, when the temperature drops to 180 °C, the GP zones are precipitated again.

(2) Due to the maximum temperature control, the alloy precipitated phases are mainly small-sized η' phases. Therefore, the strengthening mechanism of Al−Zn−Mg−Cu alloy after NIA is still mainly

precipitation strengthening.

(3) In the non-isothermal aging process, when the alloy is cooled to 140 °C, the UTS of the alloy reaches a maximum value of 582 MPa and the elongation is 11.9%.

Acknowledgments

This work was financially supported by the National Key Research and Development Program of China (No. 2018YFB2001801), the Postdoctoral Science Foundation of Central South University, China (No. 220363), and the National Natural Science Foundation of China (No. 51601229).

References

[1] AMIRI M M, FERESHTEH S F. Influence of roll speed difference on microstructure, texture and mechanical properties of 7075 aluminum plates produced via combined continuous casting and rolling process [J]. Transactions of Nonferrous Metals Society of China, 2021, 31(4): 901−912.

[2] DURSOUN T, SOUTIS C. Recent developments in advanced aircraft aluminium alloys [J]. Materials & Design, 2014, 56(4): 862−871.

[3] WEN Kai, FAN Yun-qiang, WANG Guo-jun, JIN Long-bin, LI Xi-wu, LI Zhi-hui, ZHANG Yong-an. Aging behavior and precipitate characterization of a high Zn-containing Al−Zn−Mg−Cu alloy with various tempers [J]. Materials & Design, 2016, 101: 16−23.

[4] WANG Shan-shan, JIANG Jian-tang, FAN Guo-hua, PANINDRE A M, FRANKEL G S, ZHEN Liang. Accelerated precipitation and growth of phases in an Al−Zn−Mg−Cu alloy processed by surface abrasion [J]. Acta Materialia, 2017, 131: 233−245.

[5] NAKAI M, ETO T. New aspect of development of high strength aluminum alloys for aerospace applications [J]. Materials Science and Engineering A, 2000, 285(1): 62−68.

[6] WILLIAMS J C, STARKE E A. Progress in structural materials for aerospace systems [J]. Acta Materialia, 2003, 51(19): 5775−5799.

[7] LI Yao, XU Guo-fu, LIU Shi-chao, PENG Xiao-yan, YIN Zhi-min, WANG Li, LIANG Xiao-peng. Effect of ageing treatment on fatigue crack growth of die forged Al−5.87Zn−2.07Mg−2.42Cu alloy [J]. Engineering Fracture Mechanics, 2019, 215: 251−260.

[8] KIMURA M, CHOJI M, KUSAKA M, SEO K, FUJI A. Effect of friction welding conditions and aging treatment on mechanical properties of A7075-T6 aluminium alloy friction joints [J]. Science & Technology of Welding & Joining, 2013, 10(4): 406−412.

[9] LIAO Hsueh-lung, LIN Jing-chie, LEE Sheng-long. Effect of pre-immersion on the SCC of heat-treated AA7050 in an alkaline 3.5% NaCl [J]. Corrosion Science, 2009, 51(2): 209−216.

[10] RANGANATHA R, KUMAR V A, NANDI V S, BHAT R R, MURALIDHARA B K. Multi-stage heat treatment of aluminum alloy AA7049 [J]. Transactions of Nonferrous Metals Society of China, 2013, 23(6): 1570−1575.

[11] JIANG Da-ming, LIU Yuan, LIANG Shuai, XIE Wen-long. The effects of non-isothermal aging on the strength and corrosion behavior of Al−Zn−Mg−Cu alloy [J]. Journal of Alloys and Compounds, 2016, 681: 57−65.

[12] LIU Yuan, LIANG Shuai, JIANG Da-ming. Influence of repetitious non-isothermal aging on microstructure and strength of Al−Zn−Mg−Cu alloy [J]. Journal of Alloys and Compounds, 2016, 689: 632−640.

[13] PENG Xiao-yan, LI Yao, LIANG Xiao-peng, GUO Qi, XU Guo-fu, DENG Ying, YIN Zhi-min. Precipitate behavior and mechanical properties of enhanced solution treated Al−Zn−Mg−Cu alloy during non-isothermal ageing [J]. Journal of Alloys and Compounds, 2018, 735: 964−974.

[14] HADJADJ L, AMIRA R, HAMANA D, MOSBAH A. Characterization of precipitation and phase transformations in Al−Zn−Mg alloy by the differential dilatometry [J]. Journal of Alloys and Compounds, 2008, 462(1−2): 279−283.

[15] BERG L K, GJONNES J, HANSEN V, LI X Z, KNUTSON-WEDEL M, WATERLOO G, SCHRYVERS D, WALLENBREG L R. GP-zones in Al−Zn−Mg alloys and their role in artificial aging [J]. Acta Materialia, 2001, 49(17): 3443−3451.

[16] NICOLAS M, DESCHAMPS A. Characterisation and modelling of precipitate evolution in an Al−Zn−Mg alloy during non-isothermal heat treatments [J]. Acta Materialia, 2003, 51(20): 6077−6094.

[17] AARONSON H I, KINSMAN K R, RUSSELL K C. The volume free energy change associated with precipitate nucleation [J]. Scripta Metallurgica, 1970, 4(2): 101−106.

[18] PENG Xiao-yan, LI Yao, LIANG Xiao-peng, GUO Qi, XU Guo-fu, DENG Ying, YIN Zhi-min. Precipitate behavior and mechanical properties of enhanced solution treated Al−Zn−Mg−Cu alloy during non-isothermal ageing [J]. Journal of Alloys & Compounds, 2017, 735: 964−974.

[19] BJRNEKLETT B I, GRONG, MYHR O R, KLUKEN A O. Additivity and isokinetic behaviour in relation to particle dissolution [J]. Acta Materialia, 1998, 46(17): 6257−6266.

[20] MA K, WEN H, HU T, TOPPING T D, ISHEIM D, SEIDMAN D N, LAVERNIA E J, SCHOENUNG J M. Mechanical behavior and strengthening mechanisms in ultrafine grain precipitation-strengthened aluminum alloy [J]. Acta Materialia, 2014, 62: 141−155.

[21] ARZT E. Size effects in materials due to microstructural and dimensional constraints: A comparative review [J]. Acta Materialia, 1998, 46(16): 5611−5626.

[22] LIU Yan, JIANG Da-ming, LI Bing-qing, YANG Wen-shu, HU Jie. Effect of cooling aging on microstructure and mechanical properties of an Al−Zn−Mg−Cu alloy [J]. Materials & Design, 2014, 57: 79−86.

[23] PENG Xiao-yan, GUO Qi, LIANG Xiao-peng, DENG Ying, YIN Zhi-ming. Mechanical properties, corrosion behavior and microstructures of a non-isothermal ageing treated Al−Zn−Mg−Cu alloy [J]. Materials Science and Engineering A, 2017, 688: 146−154.

非等温时效对 Al−5.87Zn−2.07Mg−2.42Cu 合金组织和性能的影响

李 耀[1]，徐国富[1,2]，彭小燕[1]，刘时超[1]，邓 英[1]，梁霄鹏[1]

1. 中南大学 材料科学与工程学院，长沙 410083；
2. 中南大学 有色金属材料科学与工程教育部重点实验室，长沙 410083

摘　要：研究 Al−5.87Zn−2.07Mg−2.42Cu 合金在非等温时效过程中组织和性能的变化，通过室温拉伸机测试合金的力学性能。结果表明，在非等温时效过程中，当合金冷却到 140 °C 时，合金的抗拉强度达到最大值(582 MPa)，此时伸长率为 11.9%。此外，通过透射电子显微镜对合金的显微组织进行观察，观察结果表明 GP 区和 η'相是合金的主要强化析出相，当合金冷却到 180 °C 时，GP 区发生二次析出。此外，经过非等温时效处理的合金的主要强化相仍为 η'相。

关键词：Al−Zn−Mg−Cu 合金；非等温时效；η'相；力学性能

(Edited by Xiang-qun LI)